Available online at www.sciencedirect.com
SCIENCE DIRECT
Geochimica et Cosmochimica Acta 70 (2006) 3059–3074
Geochimica
www.elsevier.com/locate/gca

Temperature independent thermal expansivities of calcium aluminosilicate melts between 1150 and 1973 K in the system anorthite–wollastonite–gehlenite (An–Wo–Geh): A density model

Marcel Potuzak [a,*], Mette Solvang [b], Donald B. Dingwell [a]

[a] *Department of Earth and Environmental Sciences, University of Munich, Theresienstrasse 41/III, D-80333 Munich, Germany*
[b] *Risø National Laboratory, Frederiksborgvej 399, P.O. 49, DK-4000 Roskilde, Denmark*

Received 30 June 2005; accepted in revised form 27 March 2006

Abstract

The thermal expansivities of 10 compositions from within the anorthite–wollastonite–gehlenite (An–Wo–Geh) compatibility triangle have been investigated using a combination of calorimetry and dilatometry on the glassy and liquid samples. The volumes at room temperature were derived from densities measured using the Archimedean buoyancy method. For each sample, density was measured at 298 K using glass that had a cooling-heating history of 10–10 K min^{-1}. The thermal expansion coefficient of the glass from 298 K to the glass transition interval was measured by a dilatometer and the heat capacity was measured using a differential scanning calorimeter from 298 to 1135 K. The thermal expansion coefficient and the heat flow were determined at a heating rate of 10 K min^{-1} on glasses which were previously cooled at 10 K min^{-1}. Supercooled liquid density, molar volume and molar thermal expansivities were indirectly determined by combining differential scanning calorimetric and dilatometric measurements assuming that the kinetics of enthalpy and shear relaxation are equivalent. The data obtained on supercooled liquids were compared to high-temperature predictions from the models of (Lange, R.A., Carmichael, I.S.E., 1987. Densities of Na_2O–K_2O–CaO–MgO–FeO–Fe_2O_3–Al_2O_3–TiO_2–SiO_2 liquids: New measurements and derived partial molar properties. *Geochim. Cosmochim. Acta* **51**, 2931–2946; Courtial, P., Dingwell, D.B., 1995. Nonlinear composition dependence of molar volume of melts in the CaO–Al_2O_3–SiO_2 system. *Geochim. Cosmochim. Acta* **59** (18), 3685–3695; Lange, R.A., 1997. A revised model for the density and thermal expansivity of K_2O–Na_2O–CaO–MgO–Al_2O_3–SiO_2 liquids from 700 to 1900 K: extension to crustal magmatic temperatures. *Contrib. Mineral. Petrol.* **130**, 1–11). The best linear fit combines the supercooled liquid data presented in this study and the high temperature data calculated using the Courtial and Dingwell (1995) model. This dilatometric/calorimetric method of determining supercooled liquid molar thermal expansivity greatly increases the temperature range accessible for thermal expansion. It represents a substantial increase in precision and understanding of the thermodynamics of calcium aluminosilicate melts. This enhanced precision demonstrates clearly the temperature independence of the melt expansions in the An–Wo–Geh system. This contrasts strongly with observations for neighboring system such as anorthite–diopside and raises the question of the compositional/structural origins of temperature dependence of thermal expansivity in multicomponent silicate melts.

1. Introduction

Knowledge of the thermal expansivity of silicate liquids is essential for the calculation of melt densities over the wide range of temperatures relevant for magmatic processes (Bottinga et al., 1983). Like other thermodynamic properties, the density of melts vary significantly with chemical composition as well as temperature and pressure. Thus, accurate data on the thermal expansivity of magmatic melts may play an important role in construction of PVT equations of state. Since Bottinga and Weill (1970) first suggested that the density of melts in two or three component systems could be used to determine partial molar volumes of oxide components in silicate liquids, several models based upon this approach have been proposed in the Earth science literature (Bottinga and Weill, 1970; Nelson and Carmichael, 1979; Bottinga et al., 1982; Lange and

* Corresponding author. Fax: +498921804176.
E-mail address: potuzak@min.uni-muenchen.de (M. Potuzak).

0016-7037/$ - see front matter © 2006 Elsevier Inc. All rights reserved.
doi:10.1016/j.gca.2006.03.013

Carmichael, 1987; Courtial and Dingwell, 1995; Lange, 1997; Courtial and Dingwell, 1999).

Accurate determination of liquid densities and expansivities have proved difficult owing to experimental limitations. In high-temperature buoyancy-based density measurements only restricted ranges of temperature are accessible. This is variably due to the high liquidus temperature or high superliquidus viscosity of the melt. Restricted temperature ranges result in a large uncertainty in expansivity. An example is provided by the systems Na_2O–SiO_2 and CaO–Al_2O_3–SiO_2, where, with increasing silica content, the combination of decreasing accessible temperatures and decreasing expansivities, results in error of up to several hundred percent for expansivity (Bockris et al., 1956; Courtial and Dingwell, 1995; Courtial and Dingwell, 1999). The uncertainties associated with thermal expansion of silicate liquids have been emphasized in the last few decades by several authors (e.g., Bockris et al., 1956; Bottinga, 1985; Herzberg, 1987; Lange and Carmichael, 1987; Webb, 1992; Knoche et al., 1992; Knoche et al., 1994; Lange, 1996; Lange, 1997; Gottsmann et al., 1999; Gottsmann and Dingwell, 2000; Toplis and Richet, 2000; Liu and Lange, 2001; Tangeman and Lange, 2001; Gottsmann and Dingwell, 2002; Ghiorso and Kress, 2004).

Both in industry and in nature, several processes (e.g., crystallization, crystal-melt fractionation, fragmentation of magma) occur at temperatures where a melt phase persists in metastable equilibrium at subsolidus temperatures. Dilatometry is one of the techniques which can yield expansivity, and density data, at such temperatures. However, direct determination of the expansivity of cylindrical samples just above the glass transition is difficult, since the sample will collapse under its own gravitational body forces at temperatures where the viscosity is less than 10^{11} Pa s (e.g., Tool and Eichlin, 1931; Toplis and Richet, 2000). To predict supercooled liquid expansivites from dilatometric data on cylindrical samples requires a procedure, which removes the gravitational deformation effect from the dilatometric traces. The first method was introduced by Webb et al. (1992). Supercooled liquid volumes and molar thermal expansivities are determined using scanning calorimetric and dilatometric measurements in the glassy region and at the glass transition. The extraction of supercooled liquid molar thermal expansivities from dilatometry/calorimetry is based on an assumed equivalence of the relaxation of volume and enthalpy at the glass transition. Using this technique, Knoche et al. (1992) first reported the temperature dependent expansivity of silicate melt. Recently, Sipp and Richet (2002) have provided compelling evidence in favour of the equivalence of enthalpy, volume and structural relaxation for a wide range of silicate liquid compositions. However, this procedure has met some scepticism, given that volume and enthalpy relaxation are not necessarily equivalent (Moynihan et al., 1976).

The existence of this problem led Lange (1996, 1997) to introduce an alternative method. In this method, the volume of the sample is determined at the limiting fictive temperature and combined with measurements made on the same material at superliquidus temperature. However, the calculation of molar thermal expansivity and molar volume in this way is critically dependent on precise determination of the limiting fictive temperature of the glass. In addition, Lange's method is based on indirect measurement of expansivity in the glass transition range and the values were derived just as a single V–T coordinate.

More recently, Gottsmann et al. (1999) developed a direct method to observe the thermal expansivity of a silicate melt in the relaxed liquid state. A sample is inserted within a metal container composed of a hollow cylinder and two solid cylindrical end pieces, this is then placed inside a dilatometer. The change in length of the assembly during the dilatometric measurement includes contributions from the liquid volume expansion, as well as two correction terms, one each for the expansion of the enclosing hollow cylinder and the end pieces. The reported precision of this method is about 3.5%.

Most recently, Toplis and Richet (2000) used a dilatometry technique, which was previously developed and described by (Sipp, 1998; Sipp and Richet, 2002), to determine the melt expansivity. In their study the cylindrical glassy samples were annealed isothermally until relaxation occurred with time at constant temperature. The annealing temperatures were the temperatures at which the viscosity of the samples was high enough to support the rod with which expansivity is measured. The lower part of the SiO_2 rod was in contact with the surface of the measured sample. A second SiO_2 rod was placed on a reference SiO_2 standard and the principle of differential dilatometry was applied. Despite the narrow temperature range (about 40 K), the melt expansivities were determined with a precision to within 3% and their results point to temperature dependent thermal expansivities of silicate liquids.

The results of the methods of Webb et al. (1992); Gottsmann et al. (1999) and Toplis and Richet (2000) are all in excellent agreement.

Here, we adopt the Webb et al. (1992) method to determine expansivity and volume of the calcium aluminosilicates just above the glass transition temperature. Our study has focussed on this system because these oxides are present in all natural volcanic melts and glasses and the CAS system serves as a model for experimental petrology. Horizontal dilatometry has been used to determine the density and expansivity of glassy samples, which have the same thermal history (10 K min^{-1} cooling/heating rate). Archimedean-based densitometry on separate aliquots of the samples was used to determine sample density at room-temperature. The Lange and Carmichael (1987); Lange (1997) and Courtial and Dingwell (1995) models have been used to calculate the densities of the investigated samples at superliquidus temperatures. Combining all these methods allows us to cover a wide temperature range in order to predict the molar thermal expansivity of the investigated calcium aluminosilicates.

Previous investigations of the compositional dependence of melt properties in the $CaO–Al_2O_3–SiO_2$ (CAS) system have been focused primarily on the metaluminous join $SiO_2–CaAl_2O_4$ which is highly polymerised with a nominal number of non-bridging oxygen equal to zero. In addition, recent work by Solvang et al. (2004, 2005) and Toplis and Dingwell (2004) all concentrate on the "peralkaline" field. The calcium aluminosilicate melts are important for the glass fibre industry, especially the stone wool industry (they make up to 80% of both stone wool fibres and E-glass). Understanding the physico-chemical properties and thermodynamics of the calcium aluminosilicate is crucial for optimizing the production procedures as well as for predicting fiber quality, fiber drawing ability, bio-solubility, mechanical strength of fibers and other important parameters.

The density and expansivity of 10 calcium aluminosilicate melts included in the anorthite (An) –wollastonite (Wo) –gehlenite (Geh) ($CaAl_2Si_2O_8–CaSiO_3–Ca_2Al_2SiO_7$) compatibility triangle (Fig. 1) have been investigated over a large temperature range. This study focuses on the "peralkaline" field by studying the compositional dependence of melt properties along the lines with NBO/T = 0.5 and 1. This allows us to study the effect of composition on the density and expansivity at a constant degree of polymerization and to explore the structural changes along and between the lines. So far the densities and expansivities of the melts with compositions in the An–Wo–Geh compatibility triangle have not been systematically studied.

2. Experimental

2.1. Sample preparation

Melts were synthesized from SiO_2 (Alfa Aesar, 99.9%—Ign. loss <0.3%), $CaCO_3$ (Merck, 98.5%), and Al_2O_3

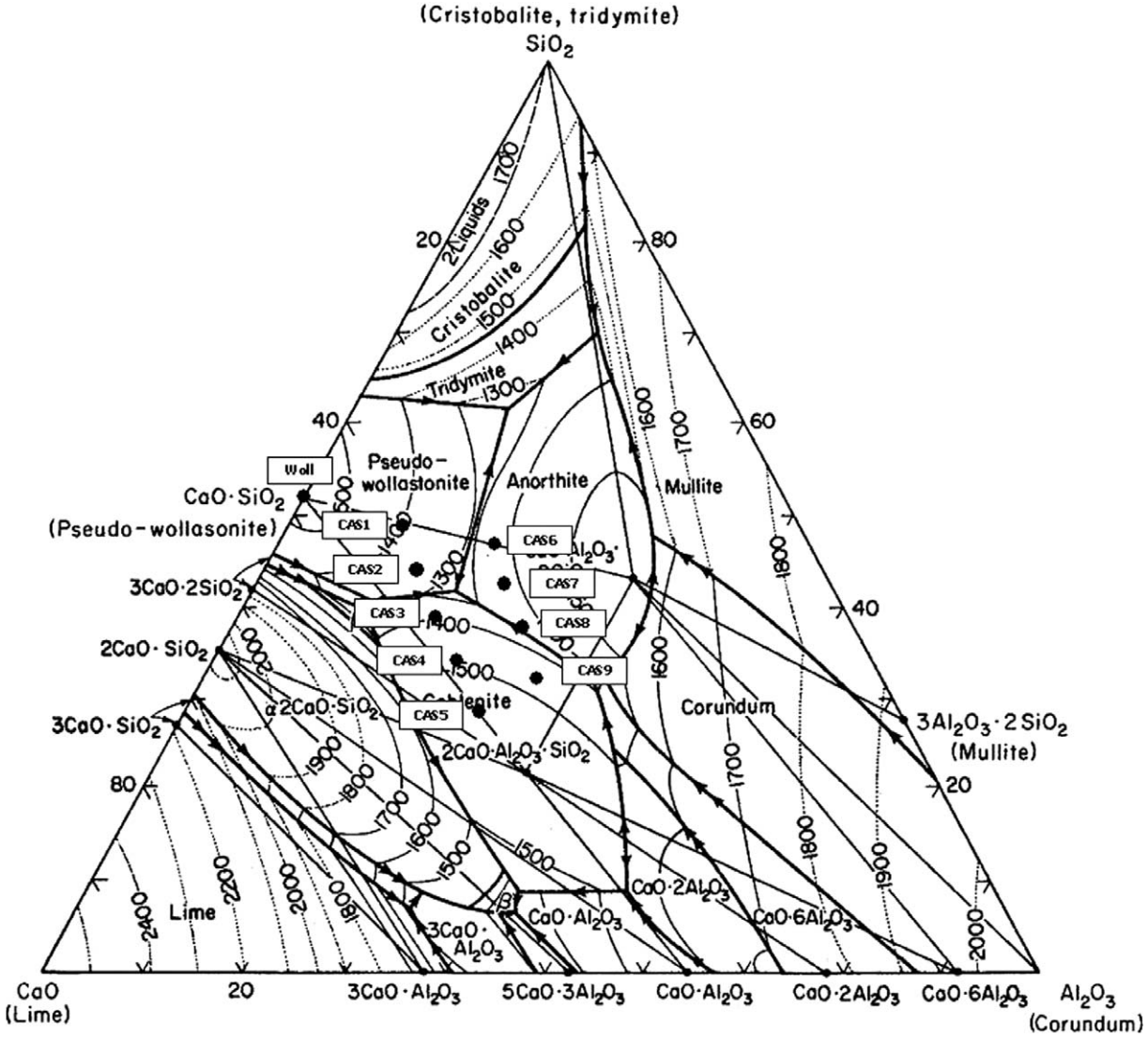

Fig. 1. Phase diagram of the $CaO–Al_2O_3–SiO_2$ (CAS) system (after Osborn and Muan, 1960; Gentile and Foster, 1963; Ehlers, 1972). The investigation deals with compositions in the anorthite–wollastonite–gehlenite (An–Wo–Ge) compatibility triangle. The compositions are in wt%. The line between CAS1 and CAS5 are the samples with NBO/T = 1 and the line between CAS6–CAS9 are the samples with NBO/T = 0.5.

(Merck, 99.9%) mixes (Fig. 1). The powders were dried at 393 K for at least 24 h prior to weighing. They were ground, mixed and then fused in a platinum crucible for 3 h in a $MoSi_2$ box furnace at 1898 K. The melts were poured from high temperature onto a stainless steel plate for cooling. A comparison between the weight of the samples before and after the melting serves as a check for the complete volatilization of CO_2 from $CaCO_3$ powder.

The high temperature viscosity was measured on the samples from 1316 to 1849 K at ambient pressure (Solvang et al., 2004). Then cylindrical bubble free glassy samples, 6 mm in diameter were drilled out from the viscometer crucible. From these cylinders glass samples for differential scanning calorimetry (DSC), dilatometry and X-ray fluorescence spectroscopy measurements were prepared and stored in a desiccator until use (Solvang et al., 2004). The compositions determined by XRF analysis (Philips 1404) are presented in Table 1. In addition, the composition of the samples that had been used in the calorimetry and dilatometry were measured by electron microprobe (CAMECA SX 50) operating under following conditions: 15 kV acceleration voltage, 10nA beam current, 20 μm defocused beam diameter, counting time 20 s on the peak and 10 s on the background. A ZAF correction was undertaken. The calibration was based on mineral standards. There were no significant differences between the composition obtained by XRF and electron microprobe analyses, both with no change from the nominal compositions (Table 1). During the various high-temperature stages of study (Solvang et al., 2004), the melts were kept in air, whereas during the low temperature experiments (i.e., DSC, dilatometry) the samples were held in a protective Ar atmosphere. There was no observable difference between the colour of the starting and the final products.

2.2. Low temperature densitometry

The room temperature densities of the glass samples were obtained by employing an Archimedean-based technique using a METTLER® Toledo balance with ethanol as the immersion liquid. The measurements were performed on the samples after the second run of dilatometry. All the samples had the same thermal history, matching cooling and heating rates of 10 K min^{-1}. The weight of each sample was measured in air and then entirely submersed in ethanol. Densities of glass samples (ρ_{glass}) were calculated using the relationship:

$$\rho_{glass} = \frac{[\rho_{ethanol}(T) * m_{air}]}{[m_{air} - m_{ethanol}]} \quad (1)$$

where m_{air} and $m_{ethanol}$ are the weights of the glass sample in air and submersed in ethanol, respectively. To account for the temperature-dependence of the density of ethanol $\rho_{ethanol}(T)$ the temperature of the immersion liquid was monitored carefully during the measurements. At least three individual measurements were conducted on the same piece of sample used to derive a standard error. The accuracy (<0.3%) of the room temperature densitometry was established by replicate measurements of commercially available standard crystals (i.e., enstatite, diopside, periclase, quartz and sapphire) and comparing them to the density data published in the literature (Cameron et al., 1973; Hazen, 1976; Haermon, 1979; Lepage et al., 1980; Sasaki et al., 1982). Results from room temperature densitometry are presented in Table 2.

Table 2
Density (g cm^{-3}) of the investigated materials at room temperature measured on glasses in air and ethanol

Sample	Temperature (K)	Density (g cm^{-3})
CAS1	298.05	2.8325 (0.0023)
CAS2	297.65	2.8504 (0.0025)
CAS3	297.65	2.8682 (0.0016)
CAS4	297.35	2.8857 (0.0028)
CAS5	297.55	2.9062 (0.0052)
CAS6	297.75	2.7627 (0.0037)
CAS7	298.05	2.7972 (0.0035)
CAS8	298.05	2.8186 (0.0038)
CAS9	298.15	2.8395 (0.0042)
Wo	298.15	2.9128 (0.0055)

The numbers within parentheses represent the errors based on the standard deviation of three replicate mass determinations.

2.3. Calorimetry

The specific heat capacities of the investigated samples were determined using a differential scanning calorimeter

Table 1
Composition of the investigated samples reported as wt% and normalized mol% of oxides

Sample	SiO_2 (wt%)	Al_2O_3 (wt%)	CaO (wt%)	Total	SiO_2 (mol%)	Al_2O_3 (mol%)	CaO (mol%)	NBO/T	*gfw* (g mol^{-1})
CAS1	47.7	13.5	38.1	99.3	49.44	8.25	42.31	1.03	61.843
CAS2	43.4	16.9	39.0	99.3	45.62	10.47	43.92	1.01	62.709
CAS3	38.8	20.2	40.4	99.4	41.28	12.66	46.05	1.00	63.544
CAS4	34.6	23.2	41.5	99.3	37.31	14.74	47.95	0.99	64.338
CAS5	30.3	25.6	43.3	99.2	33.02	16.44	50.55	1.04	64.943
CAS6	45.8	23.6	30.1	99.5	49.81	15.12	35.07	0.50	65.013
CAS7	40.0	26.8	32.6	99.4	44.09	17.41	38.50	0.54	65.833
CAS8	35.4	30.3	33.9	99.6	39.52	19.93	40.55	0.52	66.808
CAS9	30.6	33.6	35.0	99.2	34.81	22.53	42.66	0.50	67.809
Wo	50.9	0.2	48.1	99.2	49.63	0.11	50.25	2.01	58.120

The oxides were measured using XRF and are given in wt%. Data from Solvang et al. (2004, 2005).

(STA Netzsch 449C). The measurements involve a baseline measurement (two empty Pt-Rh crucibles, 6 mm in diameter, 0.1 mm wall thickness covered with a lid), sapphire standard measurement (with one crucible containing the standard and the other empty) and sample measurement (with one crucible containing the sample and the other empty). The glass sample was polished to within 1 μm to ensure an accurate fit with the bottom of the Pt-crucible and to reach a mass comparable to that of the sapphire standard (55.85 mg). Calorimetry was performed under a constant argon flow. The calorimeter was calibrated within the temperature range from 293 to 1263 K. The heat capacity (c_p) data were calculated using all the heat flow data (i.e., baseline, standard and sample) sample and standard weight and the known heat capacity of sapphire standard was taken from Robie et al. (1979). The precision of the heat capacities was ±0.7% for the glassy values and ±2% for the supercooled liquid values. The accuracy of the heat capacity of the glassy values was ±1%, and for the supercooled liquid values ±3%, respectively. Measured heat capacity of the glasses (in J g^{-1} K^{-1}) were fitted using a third order Maier and Kelley (1932) equation ($c_p = a + bT + cT^{-2}$) (Table 3). Two calorimetric measurements were made for each composition using a heating rate of 10 K min^{-1}. The first run was performed in order to relax the sample, 65–80 K above the glass transition temperature (T_g), and then cool the sample at a known rate of 10 K min^{-1}. The second run was made to determine T_g and the heat capacity where both cooling and heating rates were known (Table 4). T_g values, obtained during the second run, were taken as the peak of the specific heat capacity curve (Fig. 4). The horizontal line in Fig. 4, at a value of $3R$, is a theoretical upper limit to glassy heat capacity at constant volume (c_v), where R is the ideal gas constant. This line represents theoretical limit for a mole of isolated simple harmonic oscillators that have only vibrational degree of freedom (i.e., in the solid state). Silicate glasses have relatively small thermal expansivity, thus c_p and c_v differ by less then 1%, so this harmonic limit should also apply to c_p (i.e., heat capacities of the glasses).

The measured calorimetric results were compared with existing model of Richet (1987). The calculated values are consistent with measured c_p values (within uncertainty of DSC). The calculated c_p of glasses are higher of about 1% (absolute) for all samples except the temperature interval slightly below (~300 K) the onset temperature, where rapid increases of c_p trace can occur. The predicted c_p values are lower (~2–5%) than the measured c_p in that temper-

Table 3
Least squares fit parameters of the heat capacity glass state curves obtained using a modified Maier–Kelley equation (i.e., $c_p = a + bT + cT^{-2}$)

Sample	a	$b \times 10^{-4}$	c	R^2	Standard error	ΔT (K)
CAS1	0.92762	2.36541	−23900.795	0.99866	0.0032	298–1014
CAS2	1.00398	1.65507	−28139.408	0.99857	0.0032	298–1024
CAS3	0.91464	3.10086	−20569.448	0.99757	0.0048	298–1034
CAS4	0.94667	2.02091	−22136.687	0.99822	0.0034	298–1044
CAS5	0.89349	2.54394	−19570.683	0.99647	0.0052	298–1054
CAS6	0.95467	1.94693	−24772.988	0.99727	0.0044	298–1038
CAS7	0.90165	2.60633	−22492.289	0.99870	0.0033	298–1043
CAS8	0.94113	2.11327	−24194.172	0.99714	0.0046	298–1053
CAS9	0.98702	1.31906	−27306.309	0.99858	0.0029	298–1063
Wo	1.01636	0.59786	−33855.738	0.99901	0.0023	298–1014

Up to three different glass samples from each composition were heated at least 65 K above their T_g at 10 K min^{-1} after undergoing cooling at the same rate. From these data an average c_p was calculated (J g^{-1} K^{-1}). Regressions were performed on the average heat capacity curves of the glassy state for each composition. The onset of the glass transition area defines the high temperature end of the glassy state. ΔT is the temperature range of glassy state.

Table 4
Least squares fit parameters for $\partial L/L_0$ (cm) dilatometric traces

Samples	$a^{dil} \times 10^{-3}$	$b^{dil} \times 10^{-6}$	R^2	ΔT[a] (K)	T_g^{dil} (K)	T_g^{cal} (K)
CAS1	−2.777	8.870	0.9988	298.5–1014.5	1068	1071
CAS2	−2.785	8.969	0.9986	297.7–1024.5	1081	1082
CAS3	−2.902	9.183	0.9987	297.7–1034.5	1092	1092
CAS4	−2.940	9.311	0.9970	297.4–1044.5	1103	1103
CAS5	−2.964	9.399	0.9989	297.6–1054.5	1113	1113
CAS6	−2.420	7.422	0.9981	297.8–1038.6	1093	1096
CAS7	−2.521	7.797	0.9986	298.1–1043.5	1103	1106
CAS8	−2.577	7.946	0.9985	298.1–1053.5	1110	1111
CAS9	−2.656	8.168	0.9988	298.2–1063.3	1120	1120
Wo	−3.445	10.732	0.9992	298.2–1014.4	1065	1064

T_g temperature peaks obtained by dilatometry and calorimetry.
Linear fit parameters for $\partial L/L_0$ (cm) as a function of temperature ($\partial L/L_0 = a^{dil} + b^{dil}T$ (K)), for the investigated glasses across the temperature interval ΔT, which were heated and cooled at 10 K min^{-1} together with the glass transition temperatures obtained by dilatometry (T_g^{dil}) and calorimetry (T_g^{cal}).
[a] The upper limit of ΔT was defined by the onset of the glass transition.

ature range. An example of the predicted and measured c_p of the glass is shown on pseudo-wollastonite, CAS6 and CAS9 samples in (Fig. 4).

2.4. Dilatometry

Cylindrical, bubble-free glass samples (6 mm in diameter and 17 mm in length) were used for dilatometric investigations, the ends of which were grounded and polished to within 1 μm to ensure plane parallel surfaces. The measurements were performed using a Netzsch® DIL 402C dilatometer with a horizontal alumina-push rod. The sample assembly is supported on an alumina base connected to a measuring head. The push rod sits horizontally and is in contact with the side of the sample assembly and is also manufactured from alumina. The relative length change of the sample and alumina rod is monitored by a linear variable displacement transducer (LVDT), which is calibrated against a standard single crystal of sapphire. The reference expansivity data are taken from the National Bureau of Standards. The precision of the expansivity is $<\pm 0.1\%$, the accuracy is $<\pm 0.2\%$ for temperatures up to 1263 K. All experiments were conducted under an inert gas (Ar, the purity of Ar gas was 5.0, i.e., 99.99999%) atmosphere using a constant argon flow.

For each composition, two runs were made using heating and cooling rates of 10 K min^{-1}. The sample was heated to approximately 70 K above T_g, which corresponds to the dilatometric softening point. As with the DSC measurement the role of the first run was to relax the sample and then cool it at a known rate (10 K min^{-1}). T_g and the molar thermal expansion were found based on the results of the second run where both the cooling and heating rates were known. T_g was taken as the inflection point of the relative length change ($\partial L/L_0$) curve during the second run (Fig. 2). The inflection point corresponds to the peak point of the linear thermal expansion coefficient alpha (α_{linear}) curve as well as to the peak point of the $\partial V/\partial T$ curve as shown in Figs. 3a and b and 5. The α_{linear} is defined as the fractional increase in length (linear dimension) per unit rise in temperature. Horizontal dilatometry provide $\partial L/L_0$ (where ∂L is the increment of the change in length at a given temperature, T, and L_0 is an initial length, in cm, of the sample), as a function of temperature. The linear thermal expansion coefficient can be calculated from these dilatometric data as the relative length change of the sample per Kelvin. It is difficult to measure the relative volume expansion, therefore the linear thermal expansion coefficient is calculated as the relative change in the length across temperature interval (∂T):

$$\alpha_{\text{linear}} = \frac{1}{L_0}\frac{\partial L}{\partial T}. \tag{2}$$

The volume thermal expansion coefficient (α_{volume}) is 3 times $\alpha_{\text{linear}}(= 1/L_0(\partial L/\partial T))$ as glasses are isotropic, the linear and volume thermal expansion coefficients can be determined from one thermal expansion measurement. The thermal expansion coefficient strongly depends on the composition and temperature. The thermal expansion coefficient above the glass transition is 3–5 times larger than the one below the glass transition. The initial length and radius (r) of each sample was measured, in cm, using a micrometer, together with their mass (m) after first dilatometric measurement (i.e., after heating and cooling at known rate, 10 K min^{-1}) at room temperature (T_{room}). Using this data the length of the sample ($L(T)$) at temperature T can then be calculated by:

$$L(T) = \partial L + L_0 \tag{3}$$

and the volume ($V(T)$, cm^3) of the sample at temperature, T, by:

$$V(T) = L(T)A(T) \tag{4}$$

where $A(T) = \pi r^2$ (cross-section area of the cylindrical sample with radius, r, at temperature, T). Density (ρ, g cm^{-3}) of the sample at temperature, T, is then calculated by:

$$\rho = \frac{m}{V(T)} \tag{5}$$

where m is the initial mass of our sample (g).

Molar volume ($V_{\text{mol}}^{(T)}$, cm^3 mol^{-1}) at temperature, T, can be expressed as:

$$V_{\text{mol}}^{(T)} = V(T)\frac{gfw}{m} \tag{6}$$

where gfw is gram formula weight calculated from the composition.

The change in the molar volume of the glass with temperature is calculated at constant pressure using the molar thermal expansion coefficient ($\alpha_{\text{mol}}^{(T)}$), which can be determined using:

$$\alpha_{\text{mol}}^{(T)} = \frac{1}{V_{\text{mol\_glass}}^{(T)}}\frac{\partial V_{\text{glass}}}{\partial T} \tag{7}$$

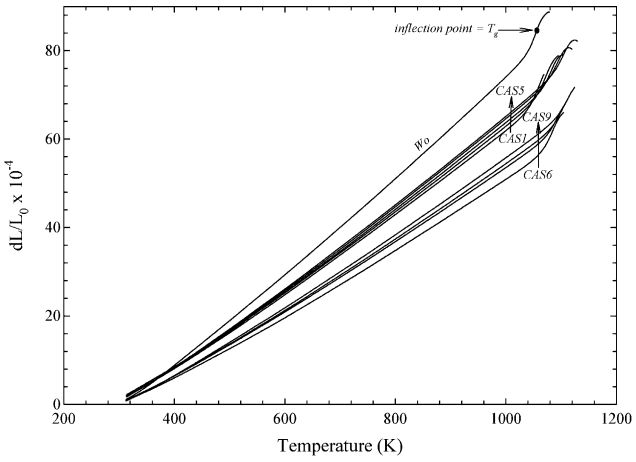

Fig. 2. dL/L_0 curves of investigated samples obtained from scanning dilatometry.

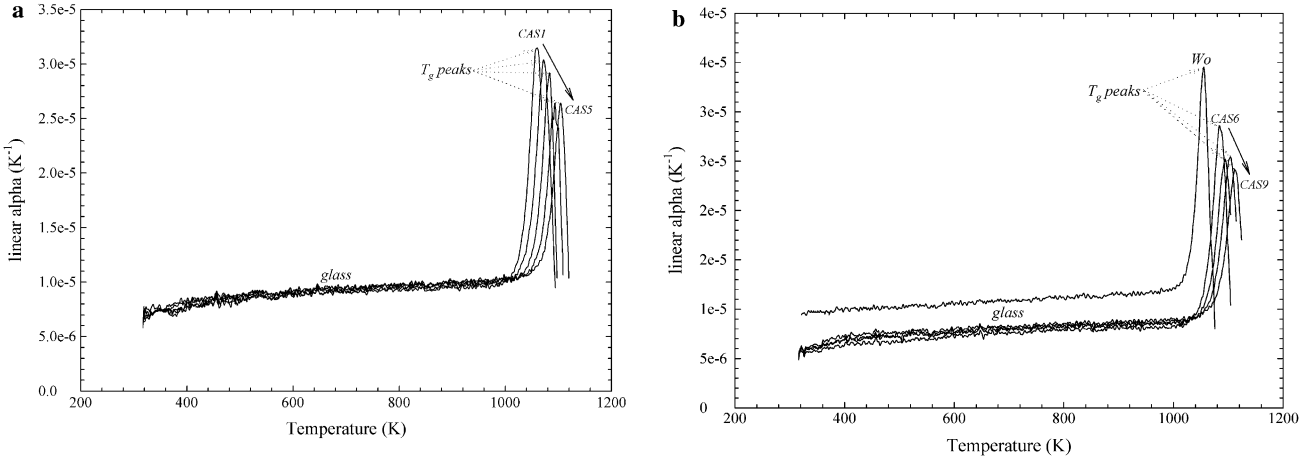

Fig. 3. Comparison of the variation of linear thermal expansion α coefficient curves as a function of temperature obtained using scanning dilatometry during the second run at a heating rate of 10 K min^{-1} for (a) samples with NBO/T = 1 (CAS1–CAS5) and (b) samples with NBO/T = 0.5 (CAS6–CAS9 and pseudo-wollastonite.

where $V^{(T)}_{\text{mol\_glass}}$ is the molar volume of the glass at temperature, T, and $\frac{\partial V_{\text{glass}}}{\partial T}$ is the molar thermal expansivity of the glass. The temperature dependence of the $\alpha^{(T)}_{\text{mol}}$ can be expressed empirically:

$$\alpha^{(T)}_{\text{mol}} = \alpha_0 + \alpha_1 T \tag{8}$$

where α_0 and α_1 are the empirical parameters. Eq. (8) assumes a linear dependency and is only a first approximation and not intended as a perfect description of the data. To obtain the temperature dependence of the molar volume of the glass, Eq. (7) is integrated between temperature, T, and 298 K using Eq. (8), one obtains Eq. (9):

$$V^{(T)}_{\text{mol\_glass}} = V^{(298)}_{\text{mol\_glass}} \exp\left[\alpha_0(T-298) + \tfrac{1}{2}\alpha_1(T^2 - 298^2)\right] \tag{9}$$

where $V^{(298)}_{\text{glass}}$ is the molar volume of the glass at room-temperature.

2.5. Combining dilatometric/calorimetric methods

Direct observation of thermal expansivity in supercooled liquids is impossible because of viscous deformation (the sharp drop in the dilatometric trace above the peak value shown in Fig. 5). In this study, the molar volume of the supercooled liquid and the molar thermal expansion of each sample across the glass transition region were calculated based on an assumed equivalence of the relaxation of volume and enthalpy at the glass transition region (i.e., Webb et al., 1992). The derivative properties (e.g., heat capacity, molar thermal expansivity) are used to reconstruct the temperature derivative of fictive temperature (T_f). T_f is defined as the contribution of the structural relaxation process to the property of interest (H or V) expressed in temperature units and may be considered as a measure of the order parameter associated with the structural relaxation process (Moynihan et al., 1976). To reconstruct the temperature derivative of T_f of any property in the glass transition interval (e.g., enthalpy, volume) the properties are normalized with respect to the temperature derivative of the liquid and glass. This normalized temperature derivative (equal to $\mathrm{d}T_f/\mathrm{d}T$) has a value of zero for the glass (i.e., T_f is constant) and 1 for the equilibrium liquid (i.e., T_f equals T). The normalized calorimetric trace is used to extend the dilatometric data of the glass into the supercooled liquid temperature range and to determine the molar thermal expansivity of the supercooled liquid across the glass transition region. Our assumption of equivalent relaxation behaviour and relaxation times for different properties has been employed and is validated by the consistency between our results and results obtained using the methods of Gottsmann and Dingwell (2000) and Toplis and Richet (2000). The observation that the peak temperature values from the calorimetric data coincide with the molar thermal expansivity calculated from dilatometric measurements dictates that insignificant viscous deformation is recorded by the dilatometer at the temperature up to the peak temperature value (Fig. 5). The derivative properties, P, (e.g., heat capacity, molar expansivity) are used to reconstruct the temperature derivative of T_f by:

$$\left.\frac{\mathrm{d}T_f}{\mathrm{d}T}\right|_T = \frac{\left[\left(\frac{\partial P}{\partial T}\right) - \left(\frac{\partial P}{\partial T}\right)_g\right]\Big|_T}{\left[\left(\frac{\partial P}{\partial T}\right)_e - \left(\frac{\partial P}{\partial T}\right)_g\right]\Big|_{T_f}} \tag{10}$$

where the subscripts e and g represent the liquid (equilibrium) and the glassy values of the property, respectively (Moynihan et al., 1976). In the present study, the enthalpy H and volume V are used as the macroscopic properties. Given the equality of the relaxation times of volume and enthalpy, Eq. (10) can be rewritten as:

$$\left.\frac{\mathrm{d}T_f}{\mathrm{d}T}\right|_T = \frac{c_p^{(T)} - c_{pg}^{(T)}}{c_{pe}^{(T_f)} - c_{pg}^{(T_f)}} = \frac{\left.\frac{\partial V^{(T)}}{\partial T} - \frac{\partial V_g^{(T)}}{\partial T}\right|_T}{\left.\frac{\partial V_e^{(T)}}{\partial T} - \frac{\partial V_g^{(T)}}{\partial T}\right|_{T_f}} \tag{11}$$

for heat capacity, c_p, and molar thermal expansivity, $\partial V/\partial T$. The behaviour of T_f in the glass transition region

can be generalized to all properties with identical relaxation times for which sufficient glassy and liquid data exist. The relaxed value of the molar thermal expansivity can now be calculated from Eq. (11).

The molar volume at the supercooled liquid temperature ($V_{\mathrm{mol}}^{T_{\mathrm{sc}}}$) just above the glass transition temperature was calculated using:

$$V_{\mathrm{mol}}^{T_{\mathrm{sc}}} = V_{\mathrm{glass}}^{(298)} + \int_{T_{\mathrm{room}}}^{T_{\mathrm{sc}}} \frac{\partial V}{\partial T} \partial T \tag{12}$$

where $V_{\mathrm{glass}}^{(298)}$ is molar volume of the sample at T_{room}. T_{sc} is the supercooled liquid temperature obtained by calorimetry and is the temperature at which stable c_p was first achieved, indicating the liquid was relaxed (Fig. 4). The molar volume at the supercooled liquid temperature ($V_{\mathrm{mol}}^{T_{\mathrm{sc}}}$) is equal to the molar volume of the glass at T_{room}($V_{\mathrm{glass}}^{(298)}$) and the area between the $\partial V/\partial T$ curve and inserted zero line at temperature range between T_{room} and T_{sc}. This volume increase was calculated in step by step manner (i.e., 0.2 K).

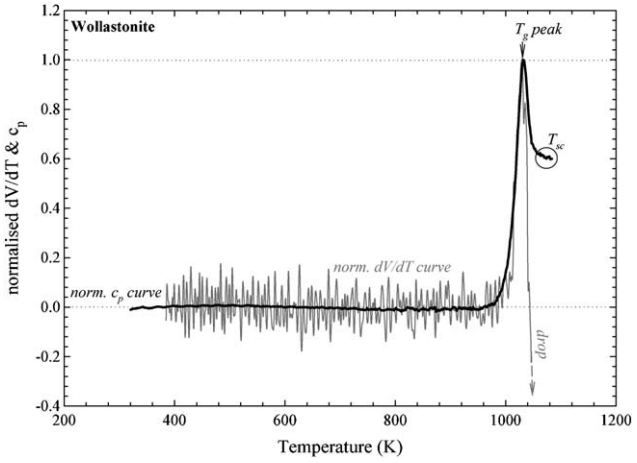

Fig. 5. The method of normalization of calorimetric and dilatometric traces illustrated for the pseudo-wollastonite sample. T_g is the glass transition temperature and T_{sc} is the temperature of the supercooled liquid.

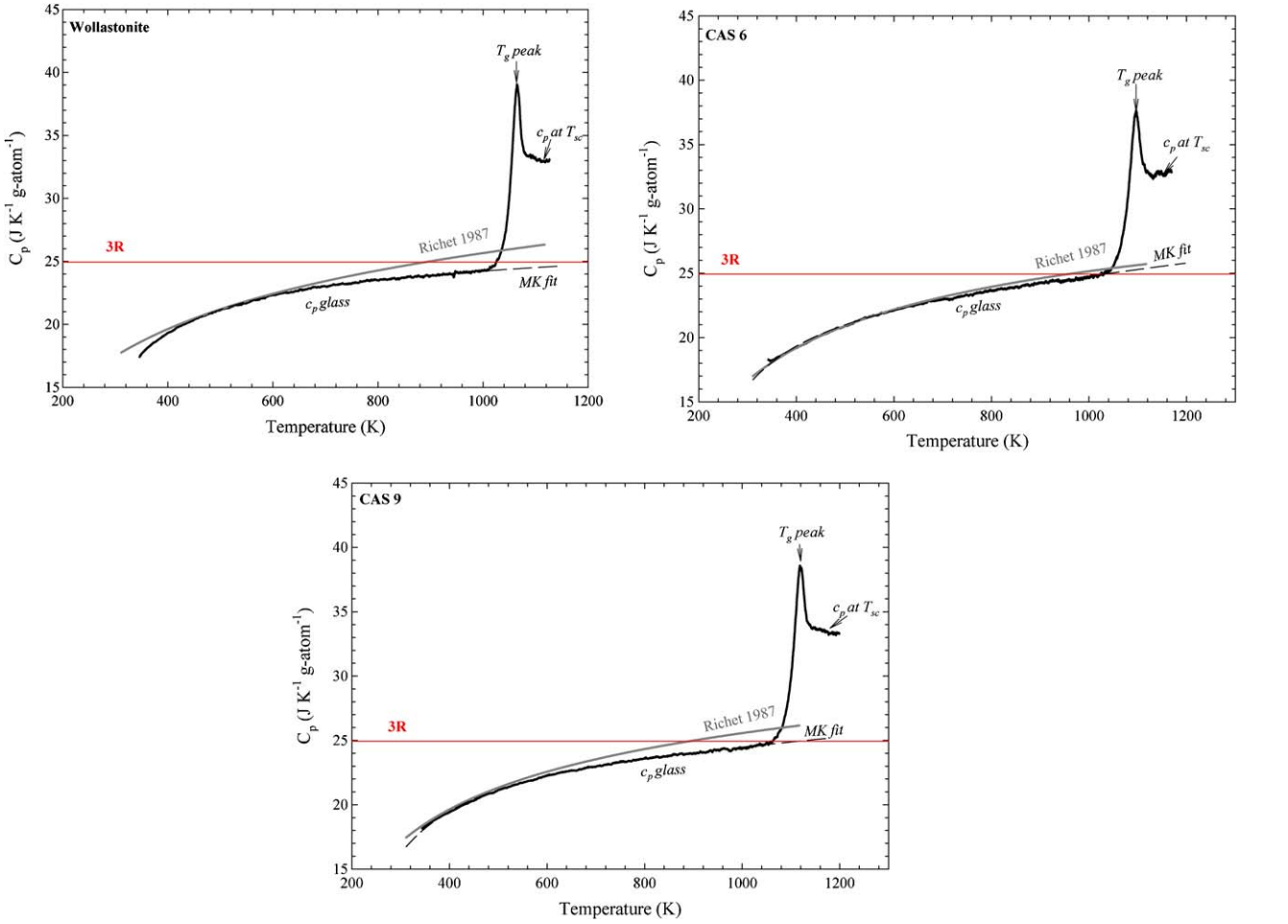

Fig. 4. Variation of heat capacity during heating across the glass transition. An examples for pseudo-wollastonite, CAS6 and CAS9. The glass transition temperature (T_g) is defined as the temperature at which the peak in heat capacity (c_p) in the glass transition occurs. The heat capacity of the glass was fitted using a third order Maier–Kelley equation, $c_p = a + bT + cT^{-2}$ (Maier and Kelley, 1932) The heat capacity of the supercooled liquid (c_p at T_{sc}) is taken as a last few points on the c_p curve, where the c_p is constant. The horizontal line, at a value of $3R$, is a theoretical upper limit to glassy heat capacities. Bold grey curve shows the calculated c_p of the glass by Richet (1987).

An example comparing normalized relaxation in the dilatometric and calorimetric traces is illustrated in Fig. 5 for the pseudo-wollastonite composition.

2.6. Partial molar volumes

The compositional dependence of the liquid molar volume is, in general, expressed by:

$$V_{\text{liquid}}(T) = \sum X_i V_i(T) \tag{13}$$

where V_{liquid} is the measured liquid molar volume, X_i the mole fraction of oxide, i, and V_i the partial molar volume of the oxide, i. This equation is valid if the molar volume has a linear variation with temperature. Courtial and Dingwell (1995) demonstrate that the molar volume exhibits non-ideal behaviour in the $CaO–Al_2O_3–SiO_2$ system, implying at least one excess term. Eq. (13) thus needs to be rewritten:

$$V_{\text{liquid}}(T) = \sum X_i V_i(T) + XS \tag{14}$$

where XS is the excess volume term corresponding to the possible interactions between SiO_2 and CaO, SiO_2 and Al_2O_3, CaO and Al_2O_3. An excess volume term between SiO_2 and CaO (XS_{SiO_2CaO}) was identified and defined as:

$$XS_{SiO_2CaO} = X_{SiO_2} X_{CaO} V_{SiO_2CaO} \tag{15}$$

where X_{SiO_2} and X_{CaO} are the molar fraction of SiO_2 and CaO, respectively, and V_{SiO_2CaO} is an excess term of these two oxides. Courtial and Dingwell (1995) tested several regression equations on the dependence of the molar volume in the $CaO–Al_2O_3–SiO_2$ system on temperature. These included an ideal models, ones with one, two and three binary excess terms. The authors recommended use of the following model, which includes an excess term between SiO_2 and CaO:

$$V_{\text{liquid}}(T) = \sum X_i \left[V_{i(1200)} + \left(\frac{\partial V_i}{\partial T} \right) (T - 1200) \right] + X_{SiO_2} X_{CaO} \left[V_{SiO_2CaO(1200)} + \left(\frac{\partial V_{SiO_2CaO(1200)}}{\partial T} \right) (T - 1200) \right] \tag{16}$$

The molar volumes of the liquids in this study were independently analysed using this equation.

The partial molar volume, molar thermal expansivity of each individual oxide and an excess term between SiO_2–CaO were obtained from two independent regressions following the model of Eq. (16). The reference temperature (1200 K) was chosen with respect to the temperature range investigated in this study. The first regression was performed on the samples used in this study. The second regression covered all the samples used in this study, together with all the CAS samples from Courtial and Dingwell (1995) and those samples with compositions relevant to the CAS system from Lange and Carmichael (1987) (samples LC3–LC8). All the samples used in the second regression contain only CaO, Al_2O_3 and SiO_2.

3. Results

3.1. Room-temperature densitometry

The densities at T_{room} of the CAS glasses from this study were measured after the dilatometric measurements. As a results, all the samples had the same cooling history (10 K min^{-1}). The density at T_{room} of samples with NBO/T = 1 (CAS1–CAS5) range from 2.8325 to 2.9062 g cm^{-3} and for samples with NBO/T = 0.5 (CAS6–CAS9) range from 2.7627 to 2.8395 g cm^{-3}. In addition, the density of pseudo-wollastonite at T_{room} was determined to be 2.9128 g cm^{-3}. Results from room temperature densitometry are presented in Table 2, showing that the density decreases greatly with increasing SiO_2 content for each of the NBO/T lines. The individual errors derived from those replicate measurements on each sample range from 0.08% to 0.19%, with the mean error being 0.12%.

3.2. Molar volume of glasses (low temperature densitometry)

The dilatometric technique allows the expansivity of the glassy samples to be measured up to the glass transition temperature.

Fig. 2 shows the second run of the dilatometric measurements as $\partial L/L_0$ for the investigated sample. The linear thermal expansion coefficient curves for all samples were obtained from the data collected during the second run of dilatometric measurements and are shown in Figs. 3a and b. The dilatometric and calorimetric glass transition temperatures, and the linear fit parameters a^{dila} and b^{dila}, which were obtained across the temperature interval ΔT, are reported in Table 4. Importantly both dilatometry and calorimetry give the same glass transition temperatures within experimental error (±3 K).

In addition, the variation of the molar volume of the glass may be approximated as a linear function of temperature, providing an average value of the molar thermal expansivity of the glass, $\overline{\partial V_{\text{glass}}/\partial T}$ (Table 5). The variable $\overline{\partial V_{\text{glass}}/\partial T}$ is equal to the regression parameter corresponding to the slope of the molar volume of the glass as a function of absolute temperature. The molar volume of the glass at (T_{room} $V^{(298)}_{\text{glass}}$) was calculated using Eq. (6). In addition, the molar volume of the glass at the given temperature (T $V^{(T)}_{\text{mol\_glass}}$) up to onset of the glass transition area is described by Eq. (9). The parameters α_0 and α_1 were obtained as the regression parameters of Eq. (9) by fitting the molar volume of the investigated glasses as a function of absolute temperature. Values of $V^{(298)}_{\text{glass}}$, $\overline{\partial V_{\text{glass}}/\partial T}$, α_0 and α_1 are listed in Table 5 for all the glasses.

The molar volume at T_{room} of samples with NBO/T = 1 (CAS1–CAS5) range from 21.833 to 22.347 $\text{cm}^3\,\text{mol}^{-1}$ and for samples with NBO/T = 0.5 (CAS6–CAS9) range from 23.532 to 23.881 $\text{cm}^3\,\text{mol}^{-1}$ (Table 5). A systematic increase in molar thermal expansivity with decreasing SiO_2

Table 5
The thermal expansion coefficients, α_0 and α_1 of the investigated glasses

Samples	V^{298}_{glass} ($cm^3\ mol^{-1}$)	$\alpha_0 \times 10^{-5}$	$\alpha_1 \times 10^{-9}$	$\overline{\partial V_{glass}/\partial T} \times 10^{-4}$ ($cm^3\ mol^{-1}\ K^{-1}$)	ΔT (K)
CAS1	21.833	2.07157	8.80637	5.847	298–1014
CAS2	22.000	2.13776	8.35953	5.958	298–1024
CAS3	22.155	2.07761	9.91997	6.145	298–1034
CAS4	22.295	2.11887	9.82553	6.270	298–1044
CAS5	22.347	2.17697	9.26436	6.346	298–1054
CAS6	23.532	1.43553	11.4702	5.268	298–1038
CAS7	23.535	1.60309	10.5976	5.536	298–1043
CAS8	23.703	1.62295	10.8624	5.683	298–1053
CAS9	23.881	1.68102	10.8296	5.887	298–1063
Wo	19.953	2.30149	13.3134	6.472	298–1014

These coefficients were obtained by performing a least squares fit of Eq. (9) in the temperature range ΔT. The molar thermal expansion coefficient α_{glass} can then be expressed empirically as $\alpha_{glass} = \alpha_0 + \alpha_1 T$ (K) within temperature range ΔT. A first approximation of the glassy molar thermal expansion $\overline{\partial V_{glass}/\partial T}$ was obtained as a regression coefficient from the linear relationship between the molar volume of the glass and absolute temperature (in the temperature range ΔT). Precise molar thermal expansion of the glass at temperature T can be calculated using Eq. (7).

content was observed for all samples irrespective of their NBO/T. Molar thermal expansivity range from 5.268×10^{-4} to $6.346 \times 10^{-4}\ cm^3\ mol^{-1}\ K^{-1}$ for all CAS samples (Table 5). Additionally, pseudo-wollastonite, which does not contain Al_2O_3 in the structure, has the lowest molar volume at T_{room} (19.953 $cm^3\ mol^{-1}$) but the highest molar thermal expansivity ($6.472 \times 10^{-4}\ cm^3\ mol^{-1}\ K^{-1}$), relative to the other investigated compositions.

3.3. Molar volume of liquids

The molar volume of the fully relaxed supercooled liquid just above the glass transition range was obtained for all investigated samples. The results derived from the normalization procedure of Webb et al. (1992) are reported in Table 6 for the T_{sc} temperature slightly higher (65–80 K) than T_g. A systematic increase in T_g with decreasing SiO_2 content is observed for both NBO/T-sets of samples. The molar volumes of the samples with the NBO/T = 1 at T_{sc} range from 22.485 to 23.010 $cm^3\ mol^{-1}$ for CAS1 and CAS5, respectively. The same trend of systematic increase in T_g with decreasing SiO_2 was also observed for samples with NBO/T = 0.5, with their molar volume ranging from 24.12 to 24.50 $cm^3\ mol^{-1}$ for CAS6 and CAS9, respectively. In addition, pseudo-wollastonite has the lowest molar volume at T_{sc}. The molar thermal expansivities of the samples with NBO/T = 1 are identical to within error. They have an average value of 17.30 $cm^3\ mol^{-1}\ K^{-1}$. The samples with NBO/T = 0.5 have a slightly lower average value of 14.20 $cm^3\ mol^{-1}\ K^{-1}$. In contrast, the molar thermal expansivity of pseudo-wollastonite is higher (20.62 $cm^3\ mol^{-1}\ K^{-1}$). The molar thermal expansion coefficients ($\alpha^{(T_{sc})}_{mol}$) of all the samples with NBO/T = 1 are roughly the same (within 0.32%) at T_{sc}, with an average of 75.954 K^{-1}. The $\alpha^{(T_{sc})}_{mol}$ for samples with NBO/T = 0.5, similarly do not vary greatly, but are slightly smaller, with an average of 58.436 K^{-1}.

The individual errors of the $V^{T_{sc}}_{mol}$ and $\alpha^{(T_{sc})}_{mol}$ determinations range from 0.04% to 0.05% and from 0.79% to 4.44%, respectively for all samples used in this study, with mean errors of 0.04% and 2.9%, respectively.

The high temperature (HT) molar volume of the investigated samples were calculated using the Lange and Carmichael (1987); Lange (1997); Courtial and Dingwell (1995) and Toplis and Richet (2000) models across the valid temperature range. The low- and high-temperature datasets were combined in order to determine the molar volumes of the samples over a very large temperature range (i.e., from the supercooled liquid up to the superliquidus liquid). The combination of the measured molar volumes at T_{sc}

Table 6
Molar volume ($cm^3\ mol^{-1}$), molar thermal expansivity ($cm^3\ mol^{-1}\ K^{-1}$) and molar thermal expansion coefficient (K^{-1}) of each melts at their supercooled liquid temperature (T_{sc}), the temperature at which the melt becomes relaxed, indicated by constant c_p

	$V^{T_{sc}}_{mol}$ ($cm^3\ mol^{-1}$)	$\frac{\partial V^{T_{sc}}}{\partial T} \times 10^{-4}$ ($cm^3\ mol^{-1}\ K^{-1}$)	$\alpha^{(T_{sc})}_{mol} \times 10^{-6}$ (K^{-1})	T_{sc} (K)	$T_{sc} - T_g$ (K)
CAS1	22.485 (0.01)	17.10	76.051 (2.1)	1150	79
CAS2	22.650 (0.01)	17.20	75.938 (1.7)	1150	68
CAS3	22.790 (0.01)	17.30	75.911 (2.2)	1160	68
CAS4	22.950 (0.01)	17.40	75.817 (0.6)	1172	69
CAS5	23.010 (0.01)	17.50	76.054 (1.5)	1178	65
CAS6	24.120 (0.01)	14.01	58.085 (2.0)	1170	74
CAS7	24.130 (0.01)	14.30	59.262 (1.9)	1180	74
CAS8	24.400 (0.01)	14.20	58.436 (2.6)	1185	74
CAS9	24.500 (0.01)	14.20	57.959 (2.4)	1200	80
Wo	20.620 (0.01)	20.50	99.418 (3.1)	1135	71

The number between the parentheses is the standard deviation from repeated measurements of the samples.

and the calculated molar volumes at superliquidus liquids is shown in Fig. 6. Linear predictions of the molar volumes at T_{sc} have been provided for all presented liquids using these three models. The molar volume predicted by the Courtial and Dingwell (1995) model at T_{sc} are in excellent agreement with the data derived for all samples from combining dilatometry and calorimetry. The molar volumes can be expressed empirically using a linear equation ($V_{mol\_liq} = a + bT(K)$) within the temperature interval ΔT. The fit parameters a and b, together with ΔT are listed in Table 7. The Courtial and Dingwell (1995) model is based on ten measurements of liquids which cover almost the entire CAS compositional range. The accessible range was controlled by the temperature of the liquidus surface and by the area of immiscibility. Their four liquid measurements are within the An–Wo–Geh system and the other three lie just outside of the system. In practice, partial molar properties are difficult to determine, especially in

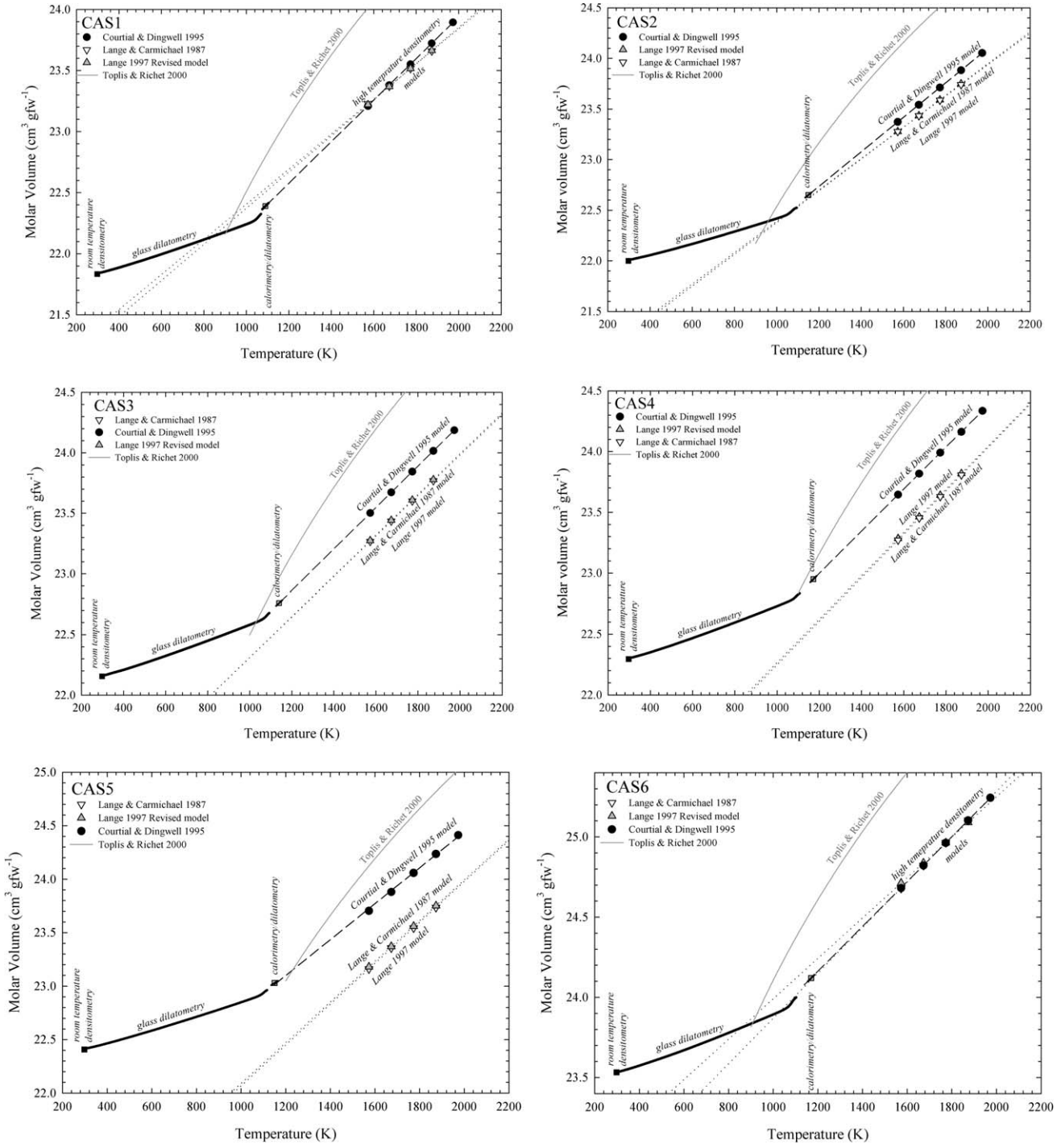

Fig. 6. Molar volume as a function of temperature for all investigated samples over the wide temperature range.

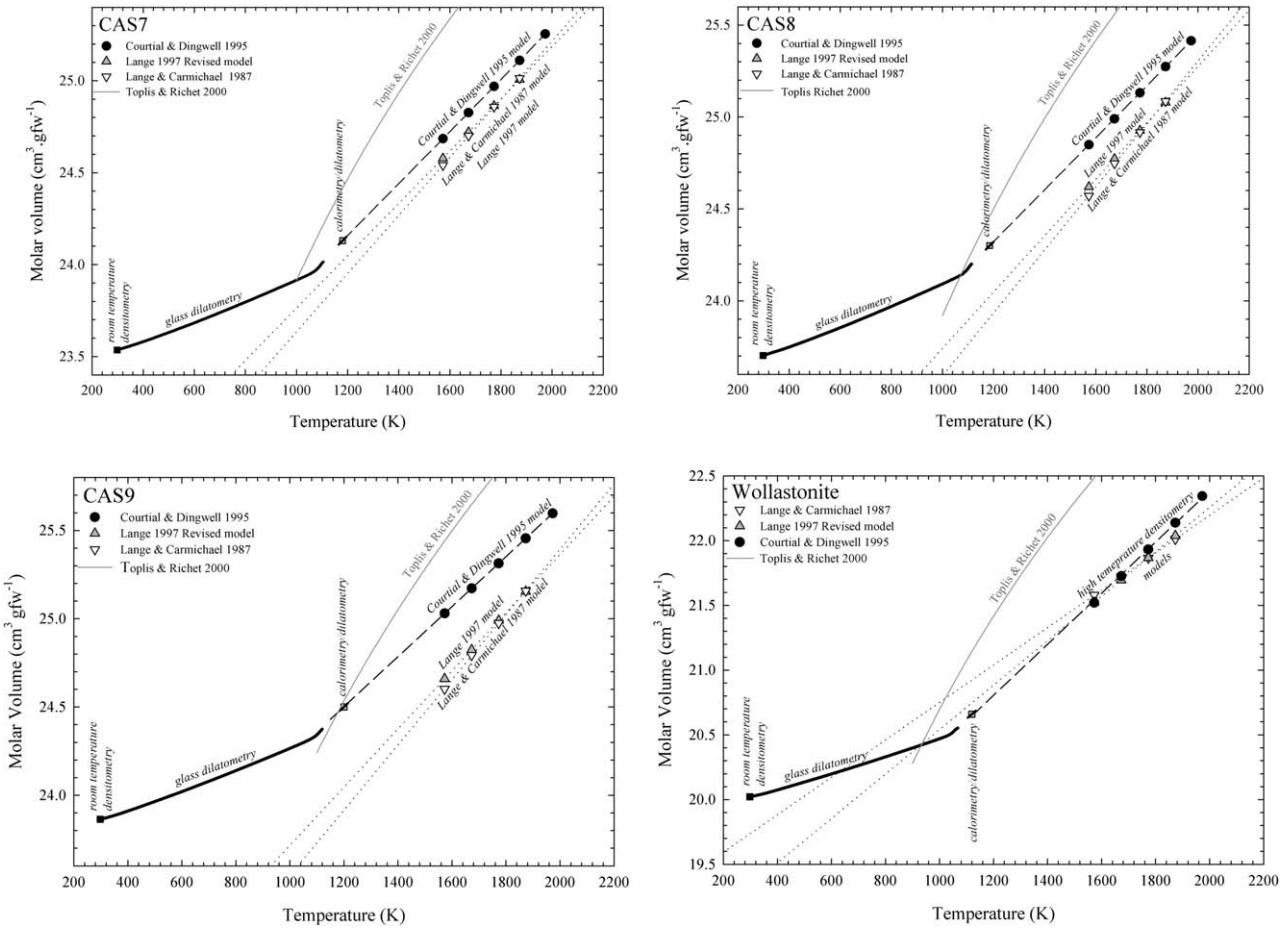

Fig. 6 (*continued*).

systems containing many components. The other models (i.e., Lange and Carmichael, 1987 and Lange, 1997) underestimate the molar volumes at T_{sc}. This results in these models overestimating the densities at T_{sc}. Only for the three compositions CAS2, CAS6 and pseudo-wollastonite does the Lange (1997) model predict the molar volume at T_{sc} to within the uncertainty of the measurements. The Toplis and Richet (2000) model is based on two liquids (i.e., anorthite and diopside) where the authors have enough volumetric data to describe them as a linear function of the logarithm of absolute temperature. The authors make the assumption that, to a first approximation, this form of temperature dependence is valid for a volumes of all liquids in the system K_2O–Na_2O–CaO–MgO–Al_2O_3–SiO_2. This model does not take into account compositional and temperature dependency of T_f. The molar volumes of our samples were calculated using the Toplis and Richet (2000) model (Fig. 6). This model overestimates the molar volumes of An–Wo–Geh melts at superliquidus temperatures. Only for the two compositions CAS4, CAS9 does the Toplis and Richet (2000) model predict the molar volume at T_{sc} or T_f within the uncertainty of the measurements. The individual errors of the molar volume predictions at T_{sc} range from 0.04% to 2.44% and from 0.03% to 2.59%, for the Lange and Carmichael (1987) model and for the Lange (1997) model, respectively.

3.4. Partial molar volumes and molar thermal expansivities

The partial molar volume (V_i) and molar thermal expansivity ($\partial V_i/\partial T$) of each individual oxide were calculated using Eq. (16). The results of two regressions following the model of Eq. (16) are reported in Table 8. Both these regressions were performed as a function of composition and temperature on all liquids over the temperature range from 1200 to 1873 K. The difference between the molar volumes of the samples calculated using the parameters listed in Table 7 and these calculated using the parameters in Table 8 is less than 0.05% for temperatures ranging from 1200 to 1873 K. The uncertainties and the quality of these regressions are indicated by the standard error of each fit coefficient (in parentheses in Table 8). The relative standard error of the regression, when compared with our experimental uncertainties, indicates whether the regression can adequately reproduce the data within our best estimate of experimental uncertainties.

The V_i and $\partial V_i/\partial T$ calculated using these regressions are directly compared with V_i and $\partial V_i/\partial T$ obtained by Lange

Table 7
Parameters to fit the linear relationship between liquid molar volume and temperature for all compositions which were obtained in temperature interval ΔT

Samples	a	$b \times 10^{-3}$	R^2	ΔT (K)
CAS1	20.532	1.703	0.9999	1150–1973
CAS2	20.690	1.704	0.9999	1150–1973
CAS3	20.808	1.712	0.9999	1160–1973
CAS4	20.924	1.729	0.9999	1172–1973
CAS5	21.084	1.679	0.9990	1178–1973
CAS6	22.486	1.396	0.9999	1170–1973
CAS7	22.457	1.417	0.9999	1180–1973
CAS8	22.624	1.415	0.9999	1185–1973
CAS9	22.801	1.417	0.9999	1200–1973
Wo	18.437	1.973	0.9994	1135–1973

The molar volumes can be expressed empirically, using $V_{\text{mol\_liq}} = a + bT\,(\text{K})$ in the temperature interval ΔT.
The lower temperature limit of ΔT is defined as the temperature of the supercooled liquid, obtained from the combined calorimetry/dilatometry method and upper temperature limit was taken as 100 K higher then the reference temperature used in the model of Courtial and Dingwell (1995).

Table 8
Regression fit parameters provided using samples molar composition to calculate partial molar volume and molar thermal expansivity of each component (i)

i	V_i, 1200 ($\text{cm}^3\,\text{mol}^{-1}$)	$\partial V_i/\partial T \times 10^{-3}$ ($\text{cm}^3\,\text{mol}^{-1}\,\text{K}^{-1}$)
1st regression		
SiO_2	27.280 (0.234)	0.000 (0.5)
Al_2O_3	36.700 (0.194)	0.000 (0.4)
CaO	19.095 (0.228)	2.033 (0.5)
SiO_2–CaO	−3.197 (0.309)	1.308 (0.6)
R^2	0.99994	
Adjusted R^2	0.99993	
S	0.0092	
2nd regression		
SiO_2	27.295 (0.396)	0.000 (0.7)
Al_2O_3	36.328 (0.352)	0.000 (0.6)
CaO	19.005 (0.248)	2.778 (0.4)
SiO_2–CaO	−3.056 (0.398)	0.121 (0.7)
R^2	0.99678	
Adjusted R^2	0.996593	
S	0.0882	

The fit parameters were derived from separate regressions of Eq. (16) for liquids in the ternary CaO–Al_2O_3–SiO_2 system (CAS). The temperature ranges from 1200 to 1873 K in steps of 100 K. V_i is the partial molar volume of component i at reference temperature 1200 K. $\partial V_i/\partial T$ is molar thermal expansivity of the component i. Note that the partial molar volumes for the first regression analysis were obtained from all our molar volume data at T_{sc} together with the HT molar volume data calculated using the model of Courtial and Dingwell (1995). In the second regression, the partial molar volumes of SiO_2, Al_2O_3, and CaO were calculated using all our molar volume data at T_{sc}, together with the HT molar volume data of our samples calculated using Courtial and Dingwell (1995) model and finally all samples relevant to CAS system used in both models of Lange and Carmichael (1987) (LC3–LC8) and Courtial and Dingwell (1995) (Ca_{YX} samples).

and Carmichael (1987); Lange (1997) and Courtial and Dingwell (1995) at the reference temperature (T_{ref}) of 1873 K in Table 9. Fitted partial molar volumes and thermal expansivities at T_{ref}. are listed in Table 9. The molar thermal expansivities of SiO_2 and Al_2O_3 are equal to zero in both provided regressions. This is in agreement with results given by Lange, 1997 model but in contrast to the results of the Lange and Carmichael (1987) and Courtial and Dingwell (1995) models. The obtained partial molar volumes of CaO are in good agreement with results of the Courtial and Dingwell (1995) model, but higher from the Lange and Carmichael (1987) and Lange (1997) models. In addition, the molar thermal expansivities of CaO obtained in both regressions are the lowest, in comparison with the other models. An excess volume term between SiO_2 and CaO can only be compared with the Courtial and Dingwell (1995) model (see Table 9).

4. Discussion

The rheological and thermodynamic properties of aluminosilicate melts are determined by the arrangement of the tetrahedral structural units in the melt, which relates to the chemical bonding situation within a structural unit and between units. Aluminum differs from silicon, since tetrahedrally coordinated aluminium is charge-balanced by either one alkali cation or half of earth alkaline cation. The charge-balancing cations for the Al^{3+} tetrahedra play a large role in the melt structure. The structural role of the alkali or earth alkaline cations commonly depends on the Al^{3+} content of the melt (Richet et al., 1993). The short range ordering in the aluminosilicate network depends on the composition and the charge-balancing or network modifying cations. For aluminosilicates it is assumed that an energetically favourably case is a random occurrence of the network forming linkages Si–O–Si, Si–O–Al and Al–O–Al. Loewenstein (1954) introduced the principle of Al-avoidance based upon consideration of mineral structures. It was postulated that the Al–O–Al linkages are energetically unfavourable. This means that the short range ordering is not random (e.g., not totally disordered). A tendency towards Al-avoidance would also appear to be the case for silicate liquids as may be inferred from thermochemical investigations (Roy and Navrotsky, 1984), NMR spectroscopy (Murdoch et al., 1985; Lee and Stebbins, 1999a,b) and variations of configurational entropy (Toplis et al., 1997). However, the presence of a small amount of Si–O–Si in glasses of anorthite compositions observed by triple quantum MAS NMR spectroscopy (Stebbins and Xu, 1997) suggests some Al–O–Al linkages (Lee and Stebbins, 1999a,b).

The investigated melts are all characterised by an excess of Ca^{2+} over the ions that act as charge-balancing for Al^{3+}. The excess of Ca^{2+} acts as a network modifier (Mysen, 1988; Sato et al., 1991; Stebbins and Xu, 1997; Cormier et al., 2000). Toplis and Dingwell (2004) discuss in detail the validity of the idea that all aluminium is associated with charge-balancing cation in peraluminous melts ($M^{n+}/n\text{Al}) \geqslant 1$. However, although Toplis and Dingwell (2004) infer that aluminosilicate melts may contain a larger number of NBO than that predicted assuming that all Al is

Table 9
Comparison of the fitted partial molar volumes and molar thermal expansivities calculated from the data presented in this study to the models of Lange and Carmichael (1987), Lange (1997) and Courtial and Dingwell (1995) at reference temperature of 1873 K

$T_{ref} = 1873$ K	V_i (cm^3 mol^{-1}) $\partial V_i/\partial T \times 10^{-3}$ (cm^3 mol^{-1} K^{-1})				
i	This study (1st regression)	This study (2nd regression)	L&C′87[a]	L′97[b]	C&D′95[c]
SiO_2	27.28	27.29	26.90	26.86	27.61
	0.00	0.00	0.00	0.00	1.85
Al_2O_3	36.70	36.33	37.63	37.42	36.36
	0.00	0.00	2.62	0.00	−2.06
CaO	20.46	20.88	17.15	17.27	20.84
	2.03	2.78	2.92	3.74	4.33
SiO_2–CaO	−2.32	−2.98	—	—	−8.35
	1.31	0.12	—	—	−4.14

[a] L&C′87—from Table 8 in Lange and Carmichael (1987).
[b] L′97—from Table 4 in Lange (1997).
[c] C&D′95—from Table 5 in Courtial and Dingwell (1995).

charge balanced (resulting in erroneous values of NBO/T). They also show that for calcium aluminosilicates this is only a major concern close to the metaluminous join where nominal NBO/T is close to zero. For the relatively depolymerised liquids considered here we have therefore calculated NBO/T using the standard calculation procedure of Mysen (1988). The deviation of NBO/T from nominal values is a complex function of the liquid composition, in particular the nature of the monovalent and divalent cations.

Solvang et al. (2004) documented a difference between the structural arrangement along the NBO/T lines = 0.5 and 1 for the identical composition as discussed in this study. The difference in structural arrangement can explain the crossover reported between the low (just above T_g) and the high viscosity data along the NBO/T = 0.5 and 1 lines. The charge-balancing cation (Ca^{2+}) have a tendency to attract the neighbouring tetrahedra of the network former, namely at the low temperature range, where the viscosity range from 10^8 to 10^{12} Pa s. Poggemann et al. (2003) confirmed that Ca^{2+} ions contract the channels in the glass network. Hence, the structural network become stronger with increasing substitution of $Al^{3+} + 1/2Ca^{2+}$ for Si^{4+}. The apparent linear dependency of the T_{room} density, molar volume of glasses (V^{298}_{glass}) and molar volume at (T_{sc} $V^{T_{sc}}_{mol}$) and T_g with increasing substitution of $Al^{3+} + 1/2Ca^{2+}$ for Si^{4+} for both NBO/T lines is a direct consequence of this structural arrangement at the low temperature range. An increase in the molar volume at both T_{room} and T_{sc} as a function of the increased substitution of $Al^{3+} + 1/2Ca^{2+}$ for Si^{4+} reflects that the structural units besides becoming stronger also favour larger clusters and hence the volume of the structural units become larger (Fig. 7a and b).

A linear temperature dependence of the molar volume between T_{sc} and the superliquidus temperature at 1 atmosphere was found for each melt. The slight increase in molar volume at T_{sc} with increasing substitution of $Al^{3+} + 1/2Ca^{2+}$ for Si^{4+} for the NBO/T = 0.5 and 1 lines, reflects increasing size of the structural units with increasing substitution, due to the role of Ca^{2+}. However, both the molar thermal expansivity and the molar thermal expansion coefficient α at T_{sc} are independent of the substitution. Both parameters (molar thermal expansivity and the molar ther-

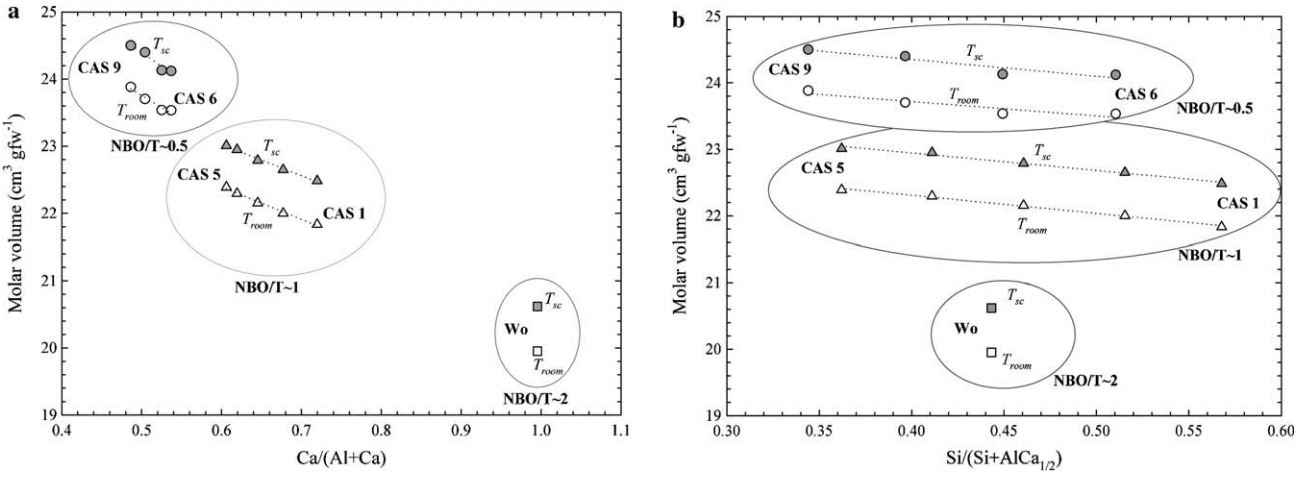

Fig. 7. Molar volume as a function of (a) Ca/(Al + Ca) ratio and (b) Si/(Si + $AlCa_{1/2}$) ratio for all investigated samples. A linear dependence is shown for each NBO-T line at supercooled liquid (T_{sc}) and room (T_{room}) temperature.

mal expansion coefficient at T_{sc}) decrease with decreasing NBO/T along the Wo–An binary join. This is a response to the change in degree of polymerisation. From Wo towards CAS6 the amount of network modifying cations decreases, and hence the liquid molar volume increases. The formation of Al–O–Si linkages in the melt decreases the amount of NBO, since the Si-NBO sites bonds are replaced by the cross-linked Al–O–Si bonds (Mysen, 1988). The most depolymerised melt (in this case Wo) has the highest molar thermal expansivity and molar thermal expansion coefficient at T_{sc}, because the NBO sites are the weakest in the silicate network (Stebbins and Xu, 1997). With increasing polymerization the Al–O–Si bonds tend to strengthen the structure and the molar thermal expansivity decreases. The change from a temperature independent thermal expansivity for wollastonite to a temperature dependent thermal expansivity for diopside (Knoche et al., 1992), despite similarity in degree of polymerisation and silica content, seems to relate to Mg content. A confirmation of such theory requires further investigation.

We would like to emphasise, that the calculation of the molar volume in a binary, ternary or multicomponent system over a wide temperature range must be treated with caution. Furthermore, it should be appreciated that the thermal expansivity is a complex function of the composition of the liquid, in particular, the nature of the cation valence. The measurements in this study have been performed at a pressure of one atmosphere. Several changes occur in the structure of silicate melts at higher pressure. For example, high coordination number of Al or hybrid structure in amorphous silicates are known to be favoured at higher pressure. These complications can cause non-ideal behaviour in the physical properties of silicate melts. As a results further spectroscopic studies, particularly at high temperature and pressure are essential. There is also lack of precise densitometry data provided on silicates with high viscosity and high melting point. This problem can be solved using a high temperature densitometry where the volume is measured on a levitated sample. Such measurements combined with in-situ spectroscopic measurements remain a challenge.

5. Conclusion

The partial molar volumes and the thermal expansivities of ten samples from within the An–Wo–Geh compatibility triangle have been determined. They have been incorporated into existing multicomponent models in order to predict silicate melt volume. The resulting supercooled liquid volumes near glass transition temperatures (1135–1200 K) and at superliquidus temperatures were combined to yield temperature independent thermal expansivities over the entire temperature range.

In light of results presented in this study, together with the published data, it seems that binary and ternary systems have temperature independent thermal expansivities from the supercooled liquid to the superliquidus temperature at 1 atmosphere. By combining the high temperature densitometry data (i.e., above liquidus) from literature with volume and expansivity data obtained at T_{sc}, a wide temperature range is covered. There is no volumetric evidence across this temperature range for temperature independent thermal expansivity in the An–Wo–Geh compatibility triangle.

Acknowledgments

We thank A.R.L. Nichols for his help to improve the manuscript. M. Potuzak has been supported by the EU Research Training Network "Volcano Dynamics" (HPRN-CT-2000-00060). M. Solvang would like also to thank Rockwool International A/S and Aalborg University, Denmark for financial support. Associated Editor J.K. Russell and three anonymous referees are thanked for careful reviews of our manuscript, which as we hope improved its clarity.

Associate editor: J. Kelly Russell

References

Bockris, J.O.M., Tomlinson, J.W., White, J.L., 1956. The structure of the liquid silicates: Partial molar volumes and expansivities. *Trans. Faraday Soc.* **53**, 299–310.

Bottinga, Y., 1985. On the isothermal compressibility of silicate liquids at high pressure. *Earth Planet. Sci. Lett.* **74** (5), 350–360.

Bottinga, Y., Richet, P., Weill, D.F., 1983. Calculation of the density and thermal expansion coefficient of silicate liquids. *Bull. Miner.* **106**, 129–138.

Bottinga, Y., Weill, D., Richet, P., 1982. Density calculations for silicate liquids.—I. Revised method for aluminosilicate compositions. *Geochim. Cosmochim. Acta* **46**, 909–919.

Bottinga, Y., Weill, D.F., 1970. Densities of liquid silicate systems calculated from partial molar volumes of oxide components. *Am. J. Sci.* **269**, 169–182.

Cameron, M., Sueno, S., Prewitt, C.T., Papike, J.J., 1973. High-temperature crystal-chemistry of Acmite, Diopside, Hedenbergite, Jadeite, Spodumene, and Ureyite. *Am. Mineral.* **58** (7–8), 594–618.

Cormier, L., Neuville, D.R., Calas, G., 2000. Structure and properties of low-silica calcium aluminosilicate glasses. *J. Non-Cryst. Solids* **274**, 110–114.

Courtial, P., Dingwell, D.B., 1995. Nonlinear composition dependence of molar volume of melts in the $CaO–Al_2O_3–SiO_2$ system. *Geochim. Cosmochim. Acta* **59** (18), 3685–3695.

Courtial, P., Dingwell, D.B., 1999. Densities of melts in the CaO–MgO–Al_2O_3–SiO_2 system. *Am. Mineral.* **84**, 465–476.

Ehlers, E.G., 1972. *The interpretation of geological phase diagrams*. W.H. Freemann and Company, San Francisco, p. 280.

Gentile, A.L., Foster, W.R., 1963. Calcium hexaluminate and its stability relations in the system $CaO–Al_2O_3–SiO_2$. *J. Am. Ceram. Soc.* **46**, 74–76.

Ghiorso, M.S., Kress, V.C., 2004. An Equation of State for Silicate Melts. II. Calibration of volumetric properties at 105 Pa. *Am. J. Sci.* **304**, 679–751.

Gottsmann, J., Dingwell, D.B., 2000. Supercooled diopside melt: confirmation of temperature-dependent expansivity using container-based dilatometry. *Contrib. Mineral. Petrol.* **139**, 127–135.

Gottsmann, J., Dingwell, D.B., 2002. Thermal expansivities of supercooled haplobasaltic liquids. *Geochim. Cosmochim. Acta* **66** (12), 2231–2238.

Gottsmann, J., Dingwell, D.B., Gennaro, C., 1999. Thermal expansion of silicate liquids: direct determination using container-based dilatometry. *Am. Mineral.* **84**, 1176–1180.

Haermon, J., 1979. The elastic constant of crystals an other anisotropic materials, In: Landolt-Börnstein tables. 1–244.

Hazen, R.M., 1976. Effects of temperature and pressure on cell dimension and X-ray temperature factors of periclase. *Am. Mineral.* **61** (3–4), 266–271.

Herzberg, C.T., 1987. Magma density at high pressure Part 1: the effect of composition on the elastic properties of silicate liquids. The Geochemical Society: Special Publication No.1, 25–46.

Knoche, R., Dingwell, D.B., Seifert, F.A., Webb, S.L., 1994. Non-linear properties of supercooled liquids in the system Na_2O–SiO_2. *Chem. Geol.* **116** (1–2), 1–16.

Knoche, R., Dingwell, D.B., Webb, S.L., 1992. Non-linear temperature dependence of liquid volumes in the system albite-anorthite-diopside. *Contrib. Mineral. Petrol.* **111**, 61–73.

Lange, R.A., 1996. Temperature independent thermal expansivities of sodium aluminosilicate melts between 713 and 1835 K. *Geochim. Cosmochim. Acta* **60** (24), 4989–4996.

Lange, R.A., 1997. A revised model for the density and thermal expansivity of K_2O–Na_2O–CaO–MgO–Al_2O_3–SiO_2 liquids from 700 to 1900 K: extension to crustal magmatic temperatures. *Contrib. Mineral. Petrol.* **130**, 1–11.

Lange, R.A., Carmichael, I.S.E., 1987. Densities of Na_2O–K_2O–CaO–MgO–FeO–Fe_2O_3–Al_2O_3–TiO_2–SiO_2 liquids: new measurements and derived partial molar properties. *Geochim. Cosmochim. Acta* **51**, 2931–2946.

Lee, S.K., Stebbins, J.F., 1999a. Al–O–Al oxygen sites in crystalline aluminates and aluminosilicate glasses: high-resolution oxygen-17 NMR results. *Am. Mineral.* **84**, 983–986.

Lee, S.K., Stebbins, J.F., 1999b. The degree of aluminum avoidance in aluminosilicate glasses. *Am. Mineral.* **84**, 937–945.

Lepage, Y., Calvert, L.D., Gabe, E.J., 1980. Parameter variation in low-quartz between 94 and 298 K. *J. Phys. Chem. Solids* **41** (7), 721–725.

Liu, Q., Lange, R.A., 2001. The partial molar volume and thermal expansivity of TiO_2 in alkali silicate melts: Systematic variation with Ti coordination. *Geochim. Cosmochim. Act* **65** (14), 2379–2393.

Loewenstein, W., 1954. The distribution of aluminum in the tetrahedra of silicates and aluminates. *Am. Mineral.* **39**, 92–96.

Maier, C.G., Kelley, K.K., 1932. An equation for the representation of high temperature heat content data. *J. Am. Ceram. Soc.* **54**, 3243–3345.

Moynihan, C.T., Easteal, A.J., Tran, D.C., Wilder, J.A., Donvan, E.P., 1976. Heat capacity and structural relaxation of mixed-alkali glasses. *J. Am. Ceram. Soc.* **59** (3–4), 137–140.

Murdoch, J.B., Stebbins, J.F., Carmichael, I.S.E., 1985. High-resolution Si-29 NMR-study of silicate and aluminosilicate glasses—the effect of network-modifying cations. *Am. Mineral.* **70**, 332–343.

Mysen, B., 1988. *Structure and Properties of Silicate Melts*. Elsevier Science Publishers BV, Amsterdam.

Nelson, S.A., Carmichael, I.S.E., 1979. Partial molar volumes of oxide components in silicate liquids. *Contrib. Mineral. Petrol.* **71**, 117–124.

Osborn, E.F., Muan, A., 1960. Phase equilibrium diagram of oxide systems. The system CaO–Al_2O_3–SiO_2. Plate1. *The American Ceramic Society and the Edward Orto Jr. Ceramic Foundation*. Columbus, Ohio.

Poggemann, J.-F., Heide, G., Frischart, G.H., 2003. Direct view of the structure of different glass fracture surfaces by atomic force microscopy. *J. Non-Cryst. Solids* **326**, 15.

Richet, P., 1987. Heat capacity of silicate glasses. *Chem. Geol.* **62**, 111–124.

Richet, P.I., Robie, R.A., Hemingway, B.S., 1993. Entropy and structure of silicate glasses and melts. *Geochim. Cosmochim. Acta* **57**, 2751–2766.

Robie, R.A., Hemingway, B.S., Fisher, J.R., 1979. *Thermodynamic properties of minerals and related substances at 298.5 K and 1 bar (10^5) Pascals and at higher temperatures*. US Government Printing Office, Washington DC, p. 456.

Roy, B.N., Navrotsky, A., 1984. Thermochemistry of charge-coupled substitutions in silicate glasses: the systems $M^{n+}_{1/n}$ AlO_2–SiO_2 (M = Li, Na, K, Rb, Cs, Mg, Ca, Sr, Ba, Pb. *J. Am. Ceram. Soc.* **67**, 606–610.

Sasaki, S., Takeuchi, Y., Fujino, K., Akimoto, S., 1982. Electron-density distributions of 3 orthopyroxenes, $Mg_2Si_2O_6$, $Co_2Si_2O_6$, and $Fe_2Si_2O_6$. *Zeitschrift Fur Kristallographie* **158** (3–4), 279–297.

Sato, R.K., McMillan, P.F., Dennison, P., Dupree, R., 1991. A structural investigation of high alumina glasses in the CaO–Al_2O_3–SiO_2 system via Raman and magic angle spinning nuclear magnetic resonance spectroscopy. *Phys. Chem. Glasses* **32** (4), 149–156.

Sipp, A., 1998. Propriétés de relaxation des silicates vitreux et fondus. PhD thesis. Université Paris VII, 231.

Sipp, A., Richet, P., 2002. Equivalence of the kinetics of volume, enthalpy and viscosity relaxation in glass forming silicate liquids. *J. Non-Cryst. Solids* **298**, 202–212.

Solvang, M., Yue, Y.Z., Jensen, S.L., Dingwell, D.B., 2004. Rheological and thermodynamic behaviors of different calcium aluminosilicate melts with the same non-bridging oxygen content. *J. Non-Cryst. Solids* **336**, 179–188.

Solvang, M., Yue, Y.Z., Jensen, S.L., Dingwell, D.B., 2005. Rheological and thermodynamic behavior of calcium aluminosilicate melts within the anorthite–wollastonite–gehlenite compatibility triangle. *J. Non-Cryst. Solids* **351**, 499–507.

Stebbins, J.F., Xu, Z., 1997. NMR evidence for excess non-bridging oxygen in an aluminosilicate glass. *Nature* **390**, 60.

Tangeman, J.A., Lange, R.A., 2001. Determination of the limiting fictive temperature of silicate glasses from calorimetric and dilatometric methods: application to the low-temperature liquid volume measurements. *Am. Mineral.* **86**, 1331–1344.

Tool, A.Q., Eichlin, C.G., 1931. Variation caused in the heating curves of glass by heat treatment. *J. Am. Ceram. Soc.* **14**, 276–308.

Toplis, M.J., Dingwell, D.B., Hess, K-U., Lenci, T., 1997. Viscosity, fragility, and configurational entropy of melts along the join SiO_2-$NaAlSiO_4$. *Am. Mineral.* **82**, 979–990.

Toplis, M.J., Richet, P., 2000. Equilibrium density and expansivity of silicate melts in the glass transition range. *Contrib. Mineral. Petrol.* **139**, 672–683.

Toplis, M.J., Dingwell, D.B., 2004. Shear viscosities of CaO–AL_2O_3–SiO_2, and MgO–Al_2O_3–SiO_2 liquids: implications for the structural role of aluminium and the degree of polymerisation of synthetic and natural aluminosilicate melts. *Geochim. Cosmochim. Acta* **68** (24), 5169–5188.

Webb, S.L., 1992. Shear, volume, enthalpy and structural relaxation in silicate melts. *Chem. Geol.* **96**, 449–457.

Webb, S.L., Knoche, R., Dingwell, D.B., 1992. Determination of silicate liquid thermal expansivities using dilatometry and calorimetry. *Eur. J. Mineral.* **4**, 95–104.